Cell PRESS
Neuron
Article

Homeostatic Regulation of AMPA Receptor Trafficking and Degradation by Light-Controlled Single-Synaptic Activation

Qingming Hou,[1] James Gilbert,[1] and Heng-Ye Man[1,*]
[1]Department of Biology, Boston University, 5 Cummington Street, Boston, MA 02215, USA
*Correspondence: hman@bu.edu
DOI 10.1016/j.neuron.2011.10.011

SUMMARY

During homeostatic adjustment in response to alterations in neuronal activity, synaptic expression of AMPA receptors (AMPARs) is globally tuned up or down so that the neuronal activity is restored to a physiological range. Given that a central neuron receives multiple presynaptic inputs, whether and how AMPAR synaptic expression is homeostatically regulated at individual synapses remain unclear. In cultured hippocampal neurons we report that when activity of an individual presynaptic terminal is selectively elevated by light-controlled excitation, AMPAR abundance at the excited synapses is selectively downregulated in an NMDAR-dependent manner. The reduction in surface AMPARs is accompanied by enhanced receptor endocytosis and dependent on proteasomal activity. Synaptic activation also leads to a site-specific increase in the ubiquitin ligase Nedd4 and polyubiquitination levels, consistent with AMPAR ubiquitination and degradation in the spine. These results indicate that AMPAR accumulation at individual synapses is subject to autonomous homeostatic regulation in response to synaptic activity.

INTRODUCTION

Homeostatic regulation as a negative feedback response lays the foundation for a large number of physiological functions including the control of body temperature, blood pressure, respiratory rhythmicity, glucose levels, osmolarity, and the pH of our bodily fluid. In the brain, developmental changes in neuronal connectivity and membrane excitability, and learning-related modification in synaptic efficacy can potentially destabilize neural network activity, leading to a state of functional saturation or silence. This potentially dysfunctional situation is believed to be prevented by a compensatory homeostatic mechanism so that a neuron's general activity, indicated by firing rate, is restrained within a certain range (Davis, 2006; Marder and Goaillard, 2006; Turrigiano, 2008). Multiple cellular targets have been implicated in the expression of homeostatic adaptation in neuronal activity including intrinsic membrane excitability, presynaptic transmitter release, balance between excitation and inhibition, synaptic depression and potentiation, as well as connectivity (Burrone and Murthy, 2003; Desai et al., 1999; Maffei and Fontanini, 2009; Pozo and Goda, 2010; Rich and Wenner, 2007; Royer and Paré, 2003; Turrigiano, 2008; Nakayama et al., 2005), but studies have revealed that homeostatic plasticity is achieved mainly through adjusting the strength of synaptic drive onto a receiving postsynaptic neuron (Burrone and Murthy, 2003; Pozo and Goda, 2010; Rabinowitch and Segev, 2008; Turrigiano, 2008). In a well-established preparation, chronic inactivation of cultured cortical neurons by TTX or TTX plus an NMDA receptor (NMDAR) antagonist APV leads to an enhancement in synaptic activity, whereas a lasting activation of network activity by blocking the inhibitory GABAA receptors weakens synaptic strength (Aoto et al., 2008; Hou et al., 2008a; Sutton et al., 2006; Turrigiano et al., 1998; Wierenga et al., 2005).

A major cellular mechanism employed for synaptic plasticity is to alter the abundance of neurotransmitter receptors at the postsynaptic domain (Collingridge et al., 2004; Malinow and Malenka, 2002; Man et al., 2000a; Newpher and Ehlers, 2008; Sheng and Hyoung Lee, 2003; Song and Huganir, 2002). In the brain most excitatory synaptic transmission is mediated by glutamatergic receptors, including AMPA receptors (AMPARs) and NMDARs. Synaptic localization of glutamate receptors can be dynamically regulated by various forms of vesicle-mediated protein trafficking, including receptor internalization, insertion, recycling, and lateral diffusion (Groc and Choquet, 2006). Not only are these dynamic processes executed to regulate but are also regulated by neuronal/synaptic activity (Collingridge et al., 2004; Malinow and Malenka, 2002; Newpher and Ehlers, 2008; Sheng and Hyoung Lee, 2003; Song and Huganir, 2002). For instance activation of glutamate receptors (Beattie et al., 2000; Ehlers, 2000) or increasing neural network activity by membrane depolarization or by unbalancing excitatory and inhibitory inputs to favor excitation (Lin et al., 2000) result in reductions in synaptic receptor accumulation through receptor internalization, whereas selective activation of synaptic NMDARs leads to facilitated AMPAR recycling and membrane insertion (Lu et al., 2001; Man et al., 2003; Park et al., 2004). Trafficking-dependent alterations in AMPAR synaptic localization serve as a primary mechanism not only for the expression of Hebbian-type synaptic plasticity (Malenka, 2003; Malinow and Malenka, 2002; Man et al., 2000a; Song and Huganir, 2002) but also for the expression of negative feedback-based homeostatic synaptic

regulation (Lévi et al., 2008; Sutton et al., 2006; Turrigiano and Nelson, 1998; Wierenga et al., 2005).

Ultimately, total receptor abundance is determined by a balance between receptor synthesis and degradation. At basal conditions, AMPARs have a half-life of about 20–30 hr (Huh and Wenthold, 1999; Mammen et al., 1997). Molecular details and signaling pathways involved in AMPAR turnover have not been well studied, but both lysosomal and proteasomal activities have been implicated in AMPAR degradation (Ehlers, 2000; Lee et al., 2004; Zhang et al., 2009). Enhanced AMPAR degradation is often observed following receptor ubiquitination and internalization (Lin et al., 2011; Lussier et al., 2011; Schwarz et al., 2010), and under certain circumstances receptor internalization is a prerequisite for degradation (Zhang et al., 2009). Furthermore, AMPARs can be synthesized locally in dendrites and spines from locally distributed receptor subunit mRNAs and protein synthesis machinery (Grooms et al., 2006; Sutton et al., 2004). Presumably, local AMPAR degradation in the spine might also occur, thereby enabling a rapid, synapse-specific adjustment in receptor abundance (Fonseca et al., 2006; Hegde, 2004; Segref and Hoppe, 2009; Steward and Schuman, 2003).

A central neuron receives thousands of inputs from presynaptic neurons distributed in a wide range of locations in the brain with varied levels of basal activity. Thus, the intensity of synaptic inputs at a neuron differs from one another, and changes from time to time depending on the cell type and local circuitry of each presynaptic neuron. Homeostatic regulation has been found to occur on the scale of neuronal networks, individual neurons (Burrone et al., 2002; Goold and Nicoll, 2010; Ibata et al., 2008), or subcellular dendritic regions (Yu and Goda, 2009); but whether it is employed at the single synapse level, crucial in our understanding of synaptic plasticity and neuronal computation as well as higher brain function, remains to be investigated. It is intriguing to postulate that an individual synapse, in a similar manner to a single neuron, has an intrinsic set point regarding its activity level, and is equipped with the molecular devices to detect it. Thus, after prolonged out-of-range synaptic activity, the individual synapse is able to autonomously adjust its strength homeostatically to the basal level. Indeed, our previous work has revealed that selective inhibition of a single synapse leads to a site-specific, homeostatic increase in AMPAR synaptic expression (Hou et al., 2008a), and the existence of homeostatic regulation at single synapses is further supported by more recent studies (Béïque et al., 2011; Lee et al., 2010). However, whether homeostatic regulation at individual synapses holds true under different circumstances, such as during excessive synaptic activation, remains unclear.

By employing engineered light-controlled glutamate receptor channels to stimulate neuronal firing (Szobota et al., 2007), we examined AMPAR accumulation at single synapses that are selectively activated by light exposure. We found that single-synaptic activation resulted in rapid AMPAR internalization, leading to a reduction in AMPAR synaptic accumulation. The removal of AMPARs required NMDAR activity but was independent of calcineurin- and NR2B NMDAR-mediated signaling. Furthermore, AMPAR removal was accompanied by enhanced protein ubiquitination and proteasomal activity at the stimulated synapses, indicating an involvement of protein degradation in the activated postsynaptic domain. These results suggest the operation of homeostatic adaption at individual synaptic sites.

RESULTS

Selective Activation of Single Synapses in Cultured Hippocampal Neurons

To selectively activate individual synapses, we employed the modified light-gated glutamate receptor GluR6 (LiGluR) to generate neuronal firing, and YFP-tagged synapsin (syn-YFP) to identify the activated axon terminals (Figure 1A). As shown in our previous work (Hou et al., 2008a), syn-YFP puncta colocalized with the endogenous presynaptic marker bassoon, and similar codistribution was found in cultures expressing syn-YFP plus LiGluR (Figure 1B, colocalization rate, syn-YFP 83.4% ± 4.1%, n = 10 fields; syn-YFP+LiGluR, 88.3% ± 3.6%, n = 10 fields). LiGluR system is based on the photoisomerization of a tethered agonist, maleimide-azobenzene-glutamate (MAG), between its *trans* and *cis* configuration. Under 380 nm ultraviolet (UV) light exposure, a switch from *trans* to *cis* mode brings MAG to the agonist binding site on LiGluR to activate the channel, which can be rapidly inactivated by 480 nm blue light to reverse the configuration back to the *trans* conformation (Szobota et al., 2007). In LiGluR-expressing neurons we found no sign of neuronal toxicity or changes in neuron morphology (Figure 1C). Axons from transfected neurons showed normal bouton structure and density (see Figure S1 available online). Immunostaining of the synaptic scaffolding protein PSD-95 revealed a synaptic localization of LiGluR (Figure 1D), suggesting that the UV-dependent neuronal firing is triggered in a physiological, synaptic-driven manner. In LiGluR-expressing neurons preincubated with agonist MAG (10 μM), whole-cell patch-clamp recordings confirmed that a brief UV exposure (1 s) could reliably induce rapid membrane depolarization, leading to lasting high-frequency firing of action potentials (Szobota et al., 2007), with an average firing rate of about 9 Hz (8.7 ± 1.3 Hz, n = 15) during the initial UV exposure (Figures 1E and 1F). Compared with low basal firing of about 0.5 Hz (0.47 ± 0.09 Hz, n = 5), UV stimulation drastically elevated neuronal activity. The membrane depolarization and firing by a single UV exposure (1 s) decayed gradually and typically ceased firing in 30–60 s. Consistent with previous work (Szobota et al., 2007), we found that UV-induced firing was reliably terminated by blue light (Figure 1G). To further confirm the UV effect, we found that in neurons expressing the calcium sensor protein GCaMP3 (Tian et al., 2009), UV exposure (1 s) induced a rapid and repeatable rise in GCaMP3 intensity (1.62 ± 0.13, n = 9), consistent with membrane depolarization and neuron activation (Figures 1H and 1I).

Because a single UV exposure triggered spiking of about 1 min or less, we adopted a protocol of UV stimulation cycles to achieve sustained firing. Throughout this study, light treatment was given as a combination of 0.3 s of blue light (480 nm) followed by 1 s of UV light (380 nm), repeated every 20 s (Figure 1J). A brief blue light was applied before UV light to reset neuronal activity in order to eliminate desensitization and ensure subsequent lasting UV-induced firing. Whole-cell recordings of LiGluR-expressing neurons revealed reliable firing by the UV stimulation protocol (Figures 2A and 2B), which was effectively

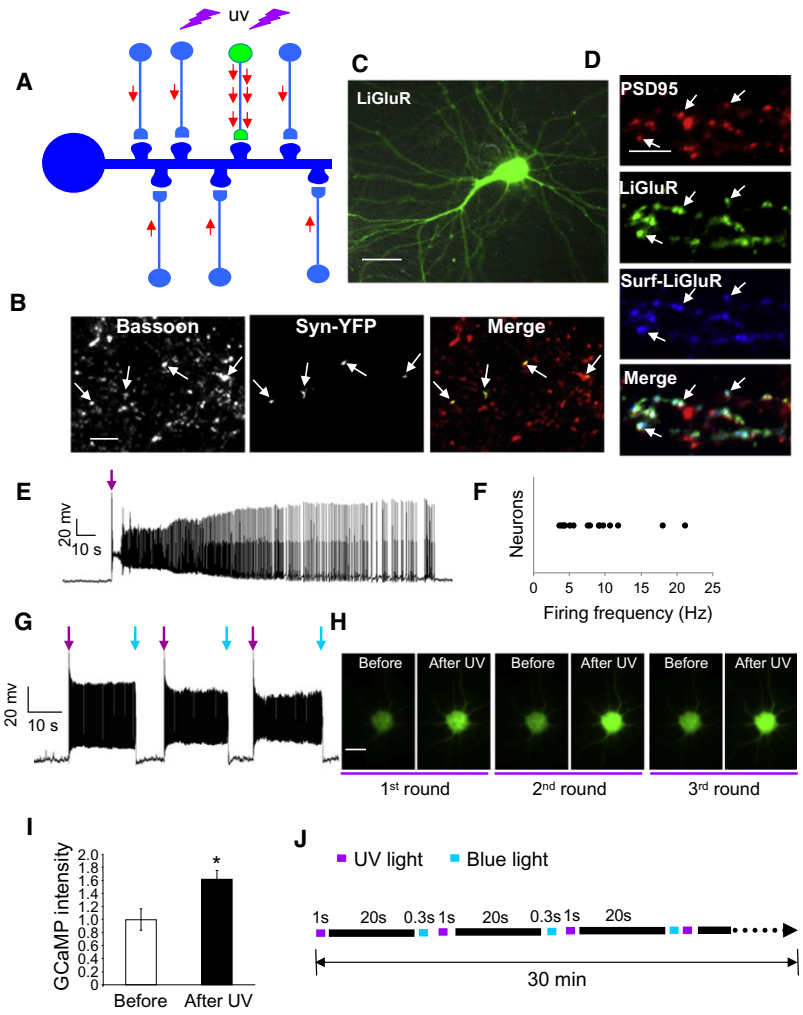

Figure 1. Light-Dependent Selective Activation of Individual Synapses in Cultured Hippocampal Neurons

(A) Schematic illustration of the experimental paradigm. In a neuronal culture network, a neuron receives multiple inputs from neighboring neurons with basal activity. Under UV stimulation the LiGluR-expressing neuron (green) was activated, thus sending more action potentials to the receiving neuron.

(B) Immunostaining of the presynaptic protein bassoon shows colocalization of syn-YFP puncta with bassoon (arrows). Scale bar, 5 μm.

(C) A 12-day-old hippocampal neuron transfected with LiGluR-GFP for 3 days shows normal healthy morphology. Scale bar, 20 μm.

(D) Colocalization of surface LiGluR with endogenous postsynaptic marker PSD-95. Transfected neurons were double stained with antibodies against surface GFP (LiGluR-GFP, blue) under nonpermeant conditions and then following permeabilization with antibodies against PSD-95 (red). Shown is a section of a dendrite. Arrows indicate puncta of colocalization. Scale bar, 5 μm.

(E and F) Whole-cell patch-clamp recording of neurons expressing LiGluR and syn-YFP. A brief UV exposure (1 s, arrow) triggered rapid depolarization and lasting firing. A plot shows variations in the firing frequency of recorded neurons (n = 15).

(G) Switching neuronal firing on and off by UV (purple arrow) and blue light (blue arrow), respectively, for three cycles.

(H and I) In a GCaMP3-expressing neuron, UV stimulation (1 s) causes a rapid rise in fluorescence intensity. Image was taken 10 s after UV exposure. Note that imaging of GFP (under blue light) terminates UV effect, recovering the GFP signal to the basal level before the 2nd and 3rd UV stimulation. Error bars, mean ± SEM. *$p < 0.05$, Student's t test. Scale bar, 20 μm.

(J) A schematic illustration of UV stimulation protocol. See also Figure S1.

blocked by AMPA/KA receptor antagonist CNQX (20 μM) (Figure S2). To confirm that neuronal activation upon UV illumination does indeed affect axonal terminal release, we performed FM4-64 uptake assays on LiGluR-expressing neurons. Transfected hippocampal neurons were incubated with LiGluR agonist MAG (10 μM) and then stimulated with UV in the presence of FM dye. Following five cycles of UV stimulation (100 s), FM intensity at terminals of LiGluR neurons (indicated by syn-YFP) was markedly enhanced compared to neighboring clusters, or syn-YFP terminals without UV treatment (Control: Neighboring sites, 372.4 ± 7.5, n = 83; LiGluR sites, 441.2 ± 18.1, n = 83, $p < 0.05$; UV treatment: Neighboring sites, 388.4 ± 10.3, n = 80; LiGluR sites, 752.3 ± 51.1, n = 80, $p < 0.05$) (Figures 2C and 2D). In contrast in the presence of TTX, UV exposure failed to increase FM labeling, indicating that the UV effect is mediated via the firing of action potentials (UV+TTX: Neighboring sites, 179.8 ± 5.4, n = 62; LiGluR sites, 193.1 ± 32.1, n = 62; $p > 0.05$) (Figures 2C and 2D). Interestingly, LiGluR terminals showed a modest but significant increase in FM intensity at basal conditions, probably due to some activation by MAG in the absence of UV, although we did not observe any change in firing rates by MAG alone. Nevertheless, terminal activity was drastically enhanced by UV exposure. We then examined FM uptake after a long-term UV stimulation, and synaptic vesicle turnover remained active following 60 cycles (20 min) of UV stimulation (Figures 2E and 2F). These results demonstrated that UV treatment could reliably cause LiGluR neurons to fire action potentials and release neurotransmitter at their axon terminals, resulting in selective activation of single synapses.

Effects of Single Synapse Activation on AMPAR Localization

We transfected 12-day-old hippocampal neurons with LiGluR together with syn-YFP. Two days after transfection, cells were incubated with MAG (10 μM) in the dark for 15 min. After washing, neurons were transferred to an imaging chamber and exposed to light treatment (blue/UV light cycles). The control neurons (transfected with LiGluR plus syn-YFP) were incubated with MAG and exposed with the same cycles of light treatment but with blue light only (0.3 s blue light followed by 1 s blue light repeated every 20 s). Both total and surface AMPAR synaptic localization were examined by immunostaining under permeant

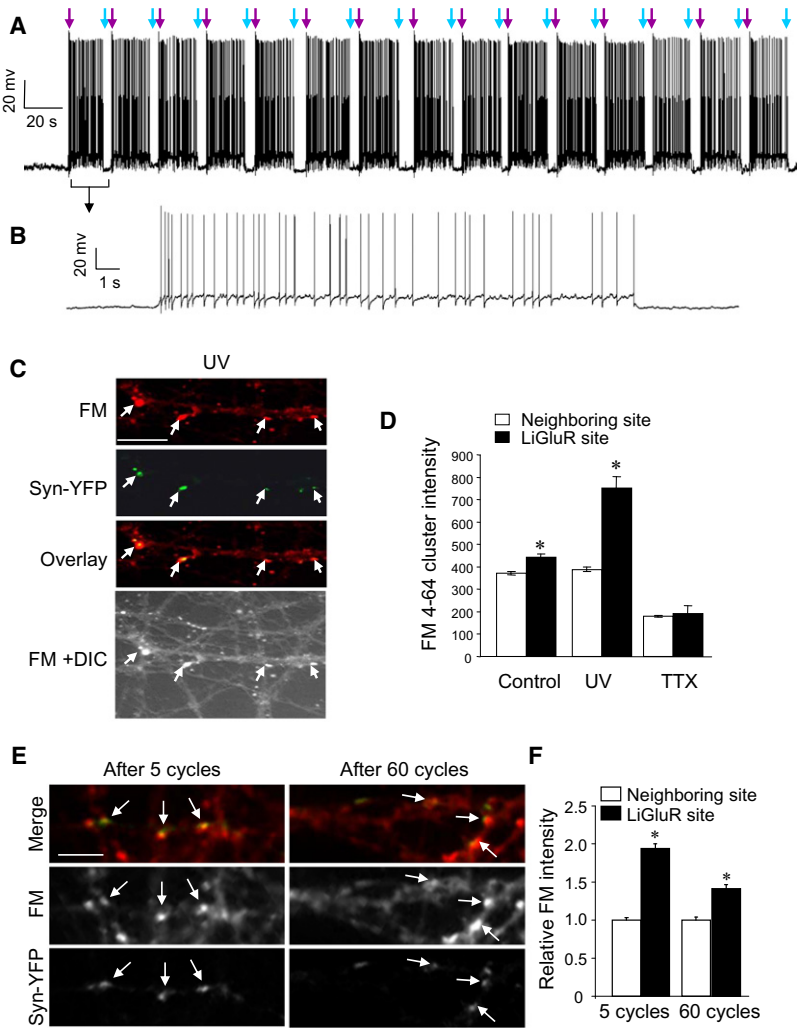

Figure 2. UV Activation of LiGluR Neurons Leads to Enhanced Presynaptic Release

(A and B) Firing pattern of a neuron expressing LiGluR and syn-YFP under UV stimulation protocol. UV-induced depolarization and firing is reset every 20 s by a brief blue light exposure. A total of 15 cycles of stimulation is shown. The first cycle of spiking is extended for clarity (B).

(C and D) Transfected 14-day-old neurons were transferred to an imaging chamber and stimulated with UV light in the presence of FM4-64 for five cycles (100 s) with or without TTX. After stimulation, neurons were washed and imaged. UV treatment dramatically increased FM intensity at the LiGluR sites, which was completely blocked by TTX. Arrows indicate puncta of colocalization.

(E and F) FM labeling after 5 and 60 cycles of UV stimulation. Following 20 min (60 cycles) of neuronal firing, neurotransmitter vesicle turnover remained significantly higher at LiGluR terminals. Arrows indicate puncta of colocalization.

Error bars, mean ± SEM. *$p < 0.05$, Student's t test. Scale bars, 5 μm.

See also Figure S2.

and nonpermeant conditions, respectively. We compared the immunofluorescence intensity of AMPAR clusters that colocalized with syn-YFP (which were from LiGluR neurons and presumably activated by UV light) to that of normal neighboring synaptic clusters. To avoid confusion with inhibitory GABAergic synapses, syn-YFP sites that showed no GluA1 immunointensity were excluded from measurements and analyses. We first examined total GluA1 accumulation at synapses using antibodies against the GluA1 extracellular N-terminal and intracellular C-terminal domains. We found that following 30 min UV photostimulation, the immunointensity of GluA1 puncta at activated synapses was significantly reduced compared with surrounding normal synapses (Total GluA1: control, 1.05 ± 0.05, n = 60; UV, 0.74 ± 0.05, n = 60; $p < 0.05$) (Figures 3A and 3C). A similar reduction was observed when we examined surface GluA1 and total GluA2/3 (GluA1 surface: control, 1.02 ± 0.06, n = 44; UV, 0.83 ± 0.06, n = 48, $p < 0.05$; GluA2/3 total: control, 0.97 ± 0.05, n = 50; UV, 0.79 ± 0.05, n = 50, $p < 0.05$) (Figures 3A–3C). In contrast in control neurons treated with only blue light, AMPAR levels at syn-YFP sites showed no difference compared to neighboring synapses. When the absolute immunointensity of GluA1 clusters was analyzed, we found a similar significant reduction in LiGluR synapses by UV activation, whereas blue light-treated controls displayed no change, indicating that the decrease of AMPAR level at activated synapses was not due to alterations of the neighboring clusters (LiGluR synapse: control, 8949 ± 819, n = 60; UV, 5693 ± 746, n = 60, $p < 0.05$; Neighboring synapse: control, 8367 ± 694, n = 60; UV, 7894 ± 868, n = 60, $p > 0.05$) (Figure 3D).

We next analyzed the synaptic intensity of another subtype of ionotropic glutamate receptor, NMDAR NR1 subunits. No difference was found in NR1 abundance at LiGluR synapses compared to that at neighboring synapses in UV-treated neurons (control, 1.01 ± 0.05, n = 66; UV, 1.09 ± 0.05, n = 66; $p > 0.05$) (Figure S3), indicating a selective regulation of AMPARs. To investigate whether synaptic scaffolding molecules were also regulated, we performed immunostaining for the postsynaptic protein PSD-95. Similar to NR1, no changes were observed in PSD abundance at the activated LiGluR synapses (control, 0.99 ± 0.06, n = 28; UV, 0.94 ± 0.07, n = 51; $p > 0.05$) (Figure S3).

We wondered whether the intensity of firing played a role in UV-induced AMPAR reduction. Because most neurons had 30–60 s of firing produced by a single UV stimulation, we used a UV stimulation protocol of 20 s intervals, so neurons basically fired continuously except for a brief 0.3 s interval gap (Figures 1E, 1G, and 2A). We found that when the stimulation interval was prolonged to 1 min, AMPAR reduction remained. However, when the UV interval was prolonged to 2 min, during which cells presumably did not fire spikes for more than half of the time, no more change in AMPAR abundance was detected at the syn-YFP synapses (1 min: control 0.97 ± 0.05, n = 46; UV 0.81 ± 0.04, n = 48, $p < 0.05$; 2 min: control 1.02 ± 0.04, n = 52;

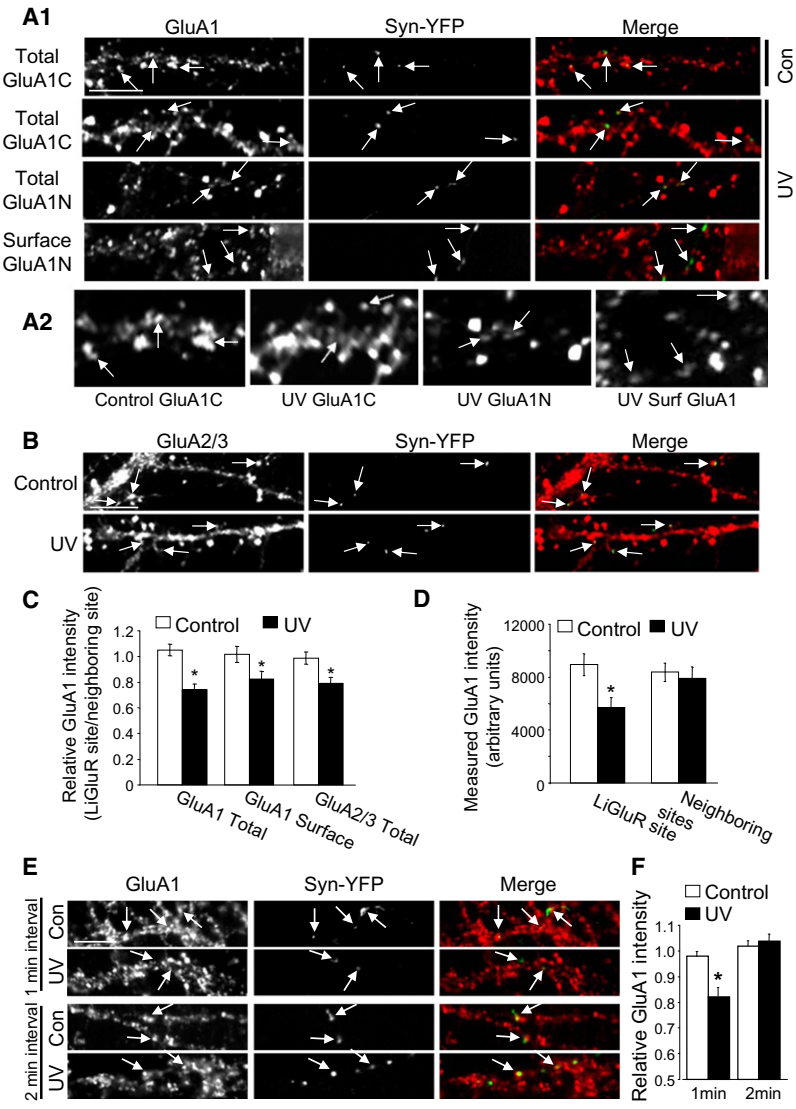

Figure 3. UV Stimulation Reduces AMPAR Abundance Selectively at LiGluR Synaptic Sites

(A) Cultured hippocampal neurons were cotransfected with syn-YFP and LiGluR. After 15 min incubation with the LiGluR agonist MAG (10 μM) in the dark, neurons were rinsed and treated with UV stimulation cycles for 30 min. GluA1 subunits were immunolabeled under permeant and nonpermeant conditions for total and surface GluA1. At LiGluR synapses, indicated by syn-YFP fluorescence (green), GluA1 immunointensity (red) was decreased following UV stimulation compared to the neighboring normal synapses. In control neurons that were exposed only to blue light without UV, AMPAR accumulation at LiGluR sites showed no change. Arrows indicate syn-YFP terminals (LiGluR sites) and the corresponding GluA1 puncta. A small region of the GluA1 image was enlarged for clarity (A2).

(B) Immunostaining of GluA2/3 under permeant conditions as in (A).

(C) Quantification of normalized intensity of total GluA1, surface GluA1, and total GluA2/3 compared to the neighboring sites.

(D) Quantification of absolute immunointensity (without normalization).

(E and F) Effect of different UV stimulation intervals. One second UV exposure for every 1 min still induced AMPAR reduction, whereas prolonged intervals of 2 min had no effect.

Error bars, mean ± SEM. *$p < 0.05$, Student's t test. Scale bars, 5 μm.

See also Figure S3.

UV 1.04 ± 0.06, n = 61, $p > 0.05$) (Figures 3E and 3F), indicating the dependency of homeostatic adjustment on the intensity and/or pattern of synaptic activity.

To obtain a dynamic picture of the redistribution of AMPARs, we measured GluA1 intensity at LiGluR sites relative to neighboring clusters following varied time periods of photostimulation. No changes were observed following 5 min of activation. At 15 min of photostimulation, GluA1 on the synaptic surface (0.84 ± 0.06, n = 33), but not its total amount (0.92 ± 0.09, n = 32), showed a marked reduction. At 30 min both surface (0.81 ± 0.07, n = 34) and total (0.77 ± 0.07, n = 33) GluA1 intensity had a 20%–25% reduction (Figures 4A–4D). This temporal sequence suggests the existence of initial receptor internalization prior to receptor removal from the spine.

NMDARs and Calcium Are Required for Activity-Dependent AMPAR Removal

To investigate the dependency of AMPAR decrease on presynaptic release and postsynaptic receptor activation, we treated transfected hippocampal neurons with various drugs 15 min before and during 30 min UV exposure. First, TTX (1 μM) was applied to block the firing of action potentials and presynaptic release. Under these conditions no difference was observed in GluA1 abundance between LiGluR synapses and their neighbors (control, 1.06 ± 0.04, n = 58; UV/TTX, 1.02 ± 0.05, n = 51; $p > 0.05$) (Figures 5A and 5B). Similarly, application of AMPA/KA receptor antagonist CNQX (20 μM) completely abolished AMPAR reduction (Figure 5B). Next, we blocked synaptic release by removing extracellular calcium. Transfected neurons were incubated in ACSF with 0 mM calcium and 1 mM of the calcium chelator EGTA. Under calcium-free conditions we found no changes in GluA1 intensity at LiGluR sites by light stimulation compared to neighboring sites, indicating the necessity of presynaptic glutamate release (UV/Ca free, 0.98 ± 0.05, n = 52; $p > 0.05$) (Figures 5A and 5B). Elevated glutamate release at activated terminals should bind to and activate postsynaptic AMPARs and NMDARs. Because stimulation of both receptors, especially NMDARs, regulates AMPAR trafficking, including receptor internalization (Lin et al., 2000), we explored the involvement of receptor activation. When LiGluR-expressing neurons were photostimulated in the presence of the NMDAR antagonist APV (50 μM), changes in GluA1 synaptic localization were completely blocked. This was in great contrast to the application of AMPAR-specific antagonist GYKI (40 μM), where the UV-induced reduction in synaptic AMPAR remained

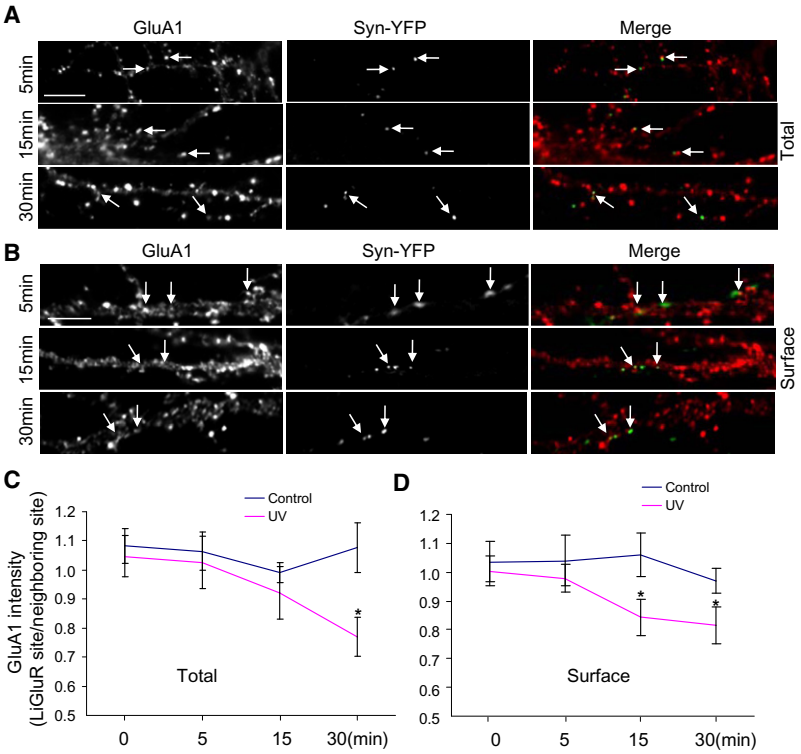

Figure 4. Time Course of Light-Induced Reduction in Synaptic GluA1 Abundance

(A and B) Transfected neurons were treated with cycles of UV light for varied periods of time. Total and surface GluA1 abundance was examined by immunostaining under permeant and nonpermeant conditions, respectively, following light stimulation. Transfected neurons receiving blue light only were used as a control. Arrows indicate puncta of colocalization. Scale bar, 5 μm.

(C and D) Quantification of time-dependent reduction of GluA1. Significant reduction in total GluA1 was not observed until 30 min of UV exposure, whereas a marked reduction in surface GluA1 was observed after 15 min of light treatment (n = 31–47 synapses from 15–20 cells, 3 independent experiments). *p < 0.05, Student's t test. Error bars, mean ± SEM.

(UV/APV, 0.94 ± 0.07, n = 53, p > 0.05; UV/GYKI, 0.85 ± 0.07, n = 50) (Figures 5A and 5B).

Light-Induced Single Synapse Activation Triggers AMPAR Internalization

We found that selective activation of LiGluR synapses by UV exposure reduced AMPAR surface localization (Figures 3A–3C). Increased neuronal activity has been shown to be a factor leading to glutamate receptor internalization (Ehlers, 2000; Lin et al., 2000), suggesting the occurrence of receptor endocytosis at activated single synapses. Therefore, we performed internalization assays to test this possibility. As described previously (Hou et al., 2008b; Man et al., 2000b, 2007), transfected neurons were incubated briefly with antibodies against the GluA1 extracellular N-terminal to label surface AMPARs. After washing, cells were transferred to an imaging chamber and photostimulated with UV for 15 min to allow receptor internalization. Following acid stripping to remove remaining surface antibodies, the internalized AMPARs were immunostained under permeant conditions. As a control, one coverslip was directly stained following antibody incubation to show total surface GluA1; another coverslip was immediately washed with acidic-stripping buffer following antibody incubation and then stained with secondary antibody under nonpermeant conditions to indicate the completeness of surface stripping. We found intensive total surface labeling and minimal fluorescence intensity in the acid-stripping control (data not shown). After 15 min UV activation, GluA1 intensity at LiGluR synapses was significantly higher compared to the surrounding unaffected synapses, indicating enhanced receptor endocytosis at activated individual synapses (control, 0.99 ± 0.07, n = 28; UV, 1.44 ± 0.13, n = 29; p < 0.05) (Figures 5C and 5D).

Homeostatic AMPAR Removal Is Not Mediated by Major Signaling Pathways Involved in AMPAR Trafficking

AMPAR trafficking is believed to be a major mechanism in the expression of traditional Hebbian plasticity, and is regulated by multiple molecules and signaling pathways. To examine whether similar regulatory processes are utilized in the activity-dependent homeostatic reduction of AMPAR at LiGluR sites, we targeted major signaling pathways known to be crucial in AMPAR endocytosis, including calcium-dependent protein phosphatase calcineurin (Beattie et al., 2000) and NR2B-NMDAR-mediated signaling (Kim et al., 2005). Surprisingly, in neurons transfected with LiGluR and syn-YFP, neither the calcineurin inhibitor FK-506 (2 μM) (control, 1.04 ± 0.07, n = 44; UV, 0.85 ± 0.07, n = 40; p < 0.05) (Figures 6A and 6D) nor the NR2B-specific inhibitor ifenprodil (5 μM) (control, 1.03 ± 0.04, n = 41; UV, 0.83 ± 0.08, n = 37; p < 0.05) (Figures 6B and 6E) blocked light-induced GluA1 reduction. In addition we also tested the role of Ca^{2+}/calmodulin-dependent protein kinase II (CaMKII), a key molecule for AMPAR surface insertion and the expression of LTP (Bredt and Nicoll, 2003). Again, no effect was found when the CaMKII inhibitor KN62 (10 μM) was applied during UV stimulation (control, 1.04 ± 0.05, n = 54; UV, 0.78 ± 0.06, n = 46; p < 0.05) (Figures 6C and 6F).

To confirm the effectiveness of these reagents, we treated neurons by brief application of NMDA (50 μM, 5 min) to induce AMPAR internalization (Beattie et al., 2000; Lee et al., 1998). We found that NMDA-induced reduction in synaptic AMPAR expression was indeed blocked by APV, FK-506, and ifenprodil (Figures S4A and S4B). Given that both NMDA application and UV stimulation trigger AMPAR endocytosis, we then tested whether they occlude each other's effect. Neurons expressing LiGluR were treated with a brief NMDA incubation (50 μM, 5 min), followed by a 30 min UV treatment in the absence of NMDA. Surface and total GluA1 were sequentially immunolabeled with anti-GluA1N and anti-GluA1C antibodies,

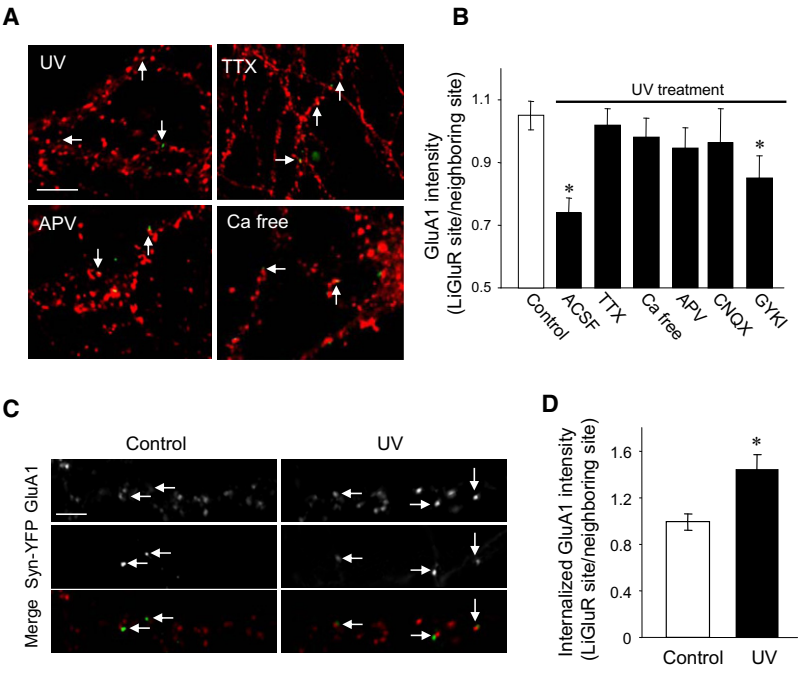

Figure 5. Involvement of NMDAR Activity and Receptor Internalization in Light-Induced AMPAR Removal

(A and B) LiGluR-expressing cells were stimulated by UV light in ACSF containing glutamate receptor antagonists APV, GYKI, and CNQX, or the sodium channel antagonist TTX, or in calcium-free ACSF. Arrows indicate puncta of colocalization.

(C and D) Internalization of AMPARs at the activated synapses. Surface AMPARs were labeled with anti-GluA1 N-terminal antibody (1:100, 3 min) at room temperature. After rinsing, neurons were treated with UV, or blue light as control, for 15 min to allow receptors to internalize. The internalized AMPARs were detected following acid stripping. In UV-treated neurons, intensity of internalized GluA1 puncta became higher than neighboring sites, indicating a selective enhancement in AMPAR internalization at the activated synapses. Arrows indicate puncta of colocalization.

Error bars, mean ± SEM. *$p < 0.05$, Student's t test. Scale bars, 5 μm.

See also Figure S4.

respectively. As expected, NMDA treatment caused a global reduction in both total and surface GluA1 cluster intensity (Total: control, 45703.9 ± 877.1, n = 2259 puncta of 13 cells; NMDA, 37309.3 ± 1038.1, n = 1765 puncta of 13 cells; Surface: control, 25539.0 ± 436.2, n = 3120 puncta of 13 cells; NMDA, 20506.2 ± 335.9, n = 3122 of 12 cells) (Figures S4C and S4D). With prior NMDA incubation a significant further reduction of GluA1 specifically at LiGluR sites was detected (Total: control, 1.11 ± 0.06, n = 37; UV, 0.85 ± 0.10, n = 32; Surface: control, 1.09 ± 0.06, n = 28; UV, 0.84 ± 0.12, n = 31) (Figures S4E and S4F), indicating that the homeostatic regulation does not completely overlap with the NMDA-dependent profile in cellular mechanisms.

Role of Proteasome-Mediated Protein Degradation in AMPAR Removal at Activated Synapses

We found that light stimulation led to a reduction in both surface and total synaptic AMPAR accumulation, and that the removal of surface receptors was likely due to receptor internalization. However, if the internalized receptors are limited within the same spine, total receptor intensity should remain largely the same. Synaptic proteins can be synthesized locally within the spine (Steward and Schuman, 2001; Tanaka et al., 2008). AMPAR subunit mRNAs have been shown to be localized and likely translated in dendrites and spines in an activity-dependent manner (Grooms et al., 2006). We reasoned that at activated individual synapses, AMPAR reduction might be a result of suppressed local protein synthesis. However, in the presence of the protein synthesis inhibitor anisomycin (30 μM) given 20 min before and during photostimulation, UV exposure still reduced AMPAR levels at activated LiGluR synapses, excluding the involvement of local protein synthesis (control, 1.07 ± 0.06, n = 53; UV, 0.72 ± 0.04, n = 44, $p < 0.05$; UV/Aniso, 0.81 ± 0.06, n = 39, $p < 0.05$) (Figures 7A and 7B).

Alternatively, synaptic AMPAR reduction might be a result of protein degradation. Indeed, AMPAR degradation subsequent to receptor trafficking has been observed upon global stimulation of glutamate receptors in cultured neurons (Ehlers, 2000; Lee et al., 2004). Internalized AMPARs can be sorted to either the recycling pool for reuse, or protein degradation machinery such as the lysosome or proteasome (Ehlers, 2000; Zhang et al., 2009, Lin et al., 2011). To determine the involvement of protein degradation, LiGluR-expressing neurons were incubated with the proteasome inhibitor MG132 (10 μM) or PR11 (0.5 μM), or the lysosome inhibitor chloroquine (200 μM) for 20 min, followed by 30 min UV stimulation in the presence of inhibitors. We found that UV activation failed to affect AMPAR abundance at the LiGluR sites in the presence of MG132 or PR11, indicating an involvement of proteasome-mediated protein degradation. In contrast, AMPAR reduction at the LiGluR sites was not affected by chloroquine, suggesting a minimal role for the lysosome (control, 1.07 ± 0.06, n = 53; UV, 0.72 ± 0.04, n = 44, $p < 0.05$; UV/MG, 1.03 ± 0.06, n = 61, $p > 0.05$; UV/Chloro, 0.89 ± 0.04, n = 51, $p < 0.05$) (Figures 7A and 7B). As a control, general GluA1 puncta intensity was measured in neurons that were treated with the degradation inhibitors for 50 min. MG132 caused a modest but significant increase, whereas no changes were detected in PR11 or chloroquine treatments (Figures S5A and S5B).

Recruitment of Ubiquitin Ligase Nedd4 but Not Proteasomes to the Activated Synapses

The ubiquitin-proteasome system (UPS) plays a key role in controlling the stability and trafficking of multiple synaptic proteins including the scaffolding proteins PSD-95, GRIP, as well as glutamate receptors (Bingol and Schuman, 2006; Ehlers, 2003; Juo and Kaplan, 2004; Kato et al., 2005; Patrick et al.,

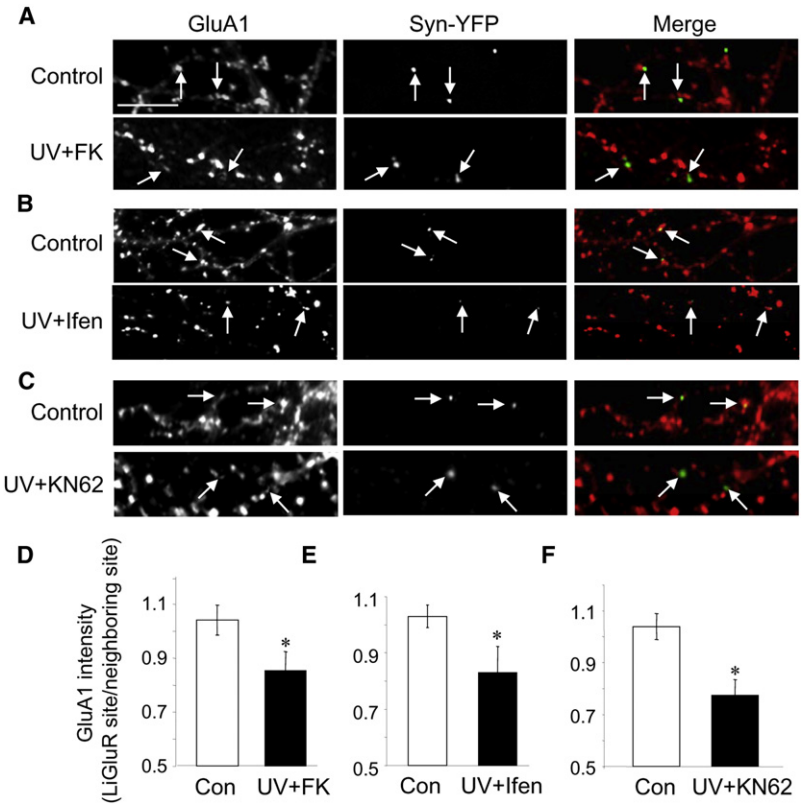

Figure 6. Major Signaling Pathways for AMPAR Trafficking Are Not Involved in Homeostatic Removal of AMPARs

Hippocampal neurons expressing LiGluR were stimulated with UV in the presence or absence of calcineurin inhibitor FK-506 (A and D), ifenprodil, an antagonist specific against NR2B-containing NMDARs (B and E), or CaMKII inhibitor KN62 (C and F). None of these inhibitors blocked UV-induced decreases in GluA1 accumulation at the activated synapses. Arrows indicate puncta of colocalization. Error bars, mean ± SEM. *$p < 0.05$, Student's t test. Scale bar, 5 μm. Con, control.

2003; Lin et al., 2011). The proteasome is distributed not only in the soma, but also in distal neurites, including dendritic spines. Interestingly, neuronal activity has been shown to induce a translocation of proteasomes into synaptic sites (Bingol and Schuman, 2006; Shen et al., 2007). We wondered whether light-induced synaptic activation leads to proteasome recruitment to the specific postsynaptic spine and, thus, facilitates receptor degradation. In cultured hippocampal neurons we first double stained the α3 subunit of the core 20S proteasome together with PSD-95 as a marker for excitatory synapses. Proteasome immunosignals showed a punctate pattern in dendrites. Consistent with previous studies (Bingol and Schuman, 2006), a large majority of proteasomal clusters colocalized with PSD-95 (data not shown), indicating an enrichment of proteasomes at synaptic sites. However, α3 immunointensity at LiGluR synapses showed no change after UV stimulation (control, 1609 ± 62, n = 83; UV, 1572 ± 58, n = 102; $p > 0.05$) (Figures 8A and 8B). We then examined the synaptic localization of ubiquitin, a short peptide whose conjugation with substrates serves as a signal for proteasomal degradation. Again, no changes were found at activated synapses (control, 2031 ± 104, n = 79; UV, 2043 ± 74, n = 100; $p > 0.05$) (Figures 8A and 8B).

Recently, the work of others and our own show that AMPARs are subject to direct ubiquitination that regulates receptor internalization and degradation (Schwarz et al., 2010; Lin et al., 2011; Lussier et al., 2011; Zhang et al., 2009). Therefore, we examined the intensity of protein ubiquitination in the spine using an antibody specific for polyubiquitin. Compared with neighboring synapses, the UV-activated synaptic sites contained higher levels of polyubiquitin signals (Figures 8C and 8D). Furthermore, because the E3 ligase Nedd4 has been shown to mediate AMPAR ubiquitination (Schwarz et al., 2010; Lin et al., 2011), we examined Nedd4 localization. Immunostaining revealed that the Nedd4 amount was significantly higher at UV-activated synapses compared to the control sites (Figures 8E and 8F), suggesting that synaptic activity recruits Nedd4 to the spine to facilitate AMPAR ubiquitination.

We found that the removal of AMPARs occurred exclusively at the light-activated synapses without affecting neighboring synapses. Furthermore, the decrease in receptor accumulation was completely blocked by inhibition of proteasomal activity, suggesting the process of local protein degradation. AMPARs have been shown to be synthesized locally at individual spines (Grooms et al., 2006; Ju et al., 2004), but whether AMPARs are subject to local protein degradation has not yet been investigated. To explore this possibility, we analyzed AMPAR turnover in dendrites isolated from the soma. In cultured hippocampal neurons transfected with GFP-GluA1, distal dendrites were separated from the soma by physical cleavage (Ju et al., 2004). Live imaging showed that 60 min following dendrite cleavage, GFP-GluA1 intensity in the isolated dendrites decreased significantly (0.78 ± 0.04, n = 6; $p < 0.05$), whereas receptors at the soma as well as proximal dendrites showed no obvious change (Figures S6A–S6C). The decrease in AMPARs at the isolated dendritic region could result from a lack of supply from the soma and ongoing local protein degradation. Indeed, when the proteasome inhibitor MG132 was applied 15 min prior to and following dendrite cleavage, no obvious change in GFP-GluA1 intensity was observed at isolated dendrites (0.99 ± 0.03, n = 5; $p > 0.05$) (Figures S6A and S6C). Next, we performed similar experiments in neuronal cultures that were transfected with syn-YFP and LiGluR. Following cleavage of dendrites of non-transfected neurons, cells were treated with UV alone or in the presence of MG132. Immunostaining showed that GluA1 levels at LiGluR synapses were reduced in both intact and isolated dendrites (Intact dendrites: 0.76 ± 0.04, n = 39, $p < 0.05$; Isolated dendrites: 0.86 ± 0.06, n = 39, $p < 0.05$). Also, consistent with receptor degradation, GluA1 reduction was completely blocked

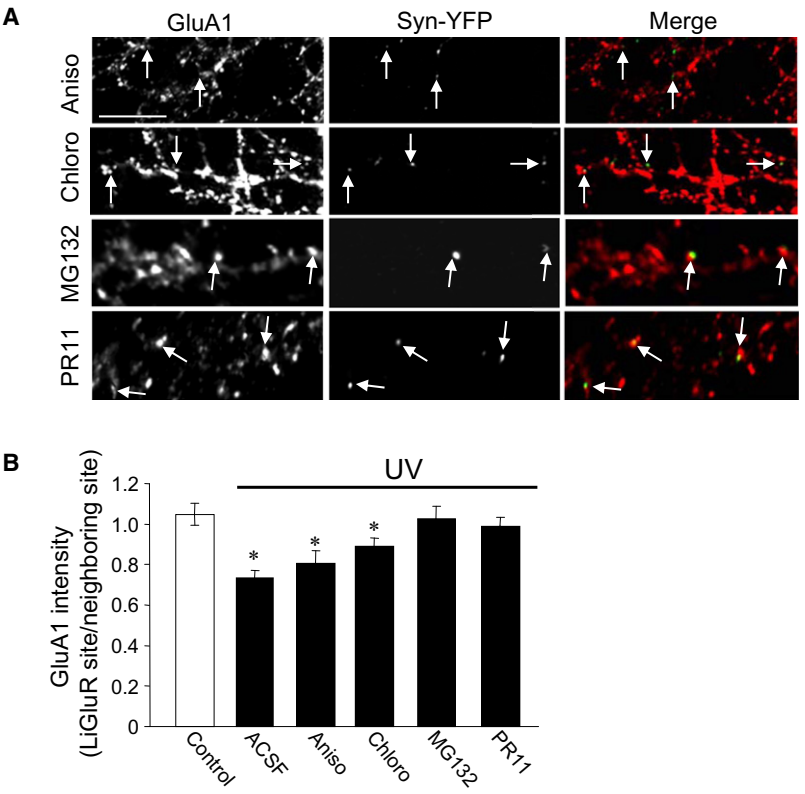

Figure 7. Proteasome-Mediated AMPAR Degradation at Light-Activated Single Synapses

(A and B) In the presence of the protein synthesis inhibitor anisomycin (Aniso, 30 μM), UV stimulation still induced GluA1 reduction at LiGluR synapses. In contrast, application of the proteasome-specific inhibitor MG132 (MG, 10 μM) and PR11 (0.5 μM), but not the lysosome inhibitor chloroquine (Chloro, 200 μM), blocked the UV effect. Arrows indicate puncta of colocalization. Error bars, mean ± SEM. *p < 0.05, Student's t test. Scale bar, 5 μm. See also Figure S5.

by MG132 (Intact dendrites: 0.99 ± 0.05, n = 44, p > 0.05; Isolated dendrites: 1.02 ± 0.05, n = 44, p > 0.05) (Figures S6D and S6E). These results suggest that AMPARs can be degraded by proteasomes residing locally in the dendrites or spines independent of the soma, consistent with the aforementioned data showing local accumulation of the ubiquitin ligase Nedd4 and polyubiquitinated proteins in activated spines.

DISCUSSION

We have demonstrated that light stimulation selectively activates LiGluR-expressing neurons and enhances presynaptic terminal activity. By identifying targeted single synapses via the fluorescence-tagged presynaptic marker protein syn-YFP, we were able to examine changes in AMPAR abundance at the activated synapses compared to intact neighboring sites. We found that the abundance of AMPARs at activated synapses was homeostatically downregulated. Although NMDARs are usually closely colocalized with AMPARs at the same synapses, light-controlled synaptic activity showed no effect on NMDAR accumulation, indicating high specificity in targeting receptors for modification.

Receptor downregulation following single-synaptic activation occurs on both surface and intraspinal AMPARs. Whereas receptor internalization is likely the reason for the reduction in surface AMPAR expression, it cannot account for the reduction in total receptor abundance at the activated synapses. We found

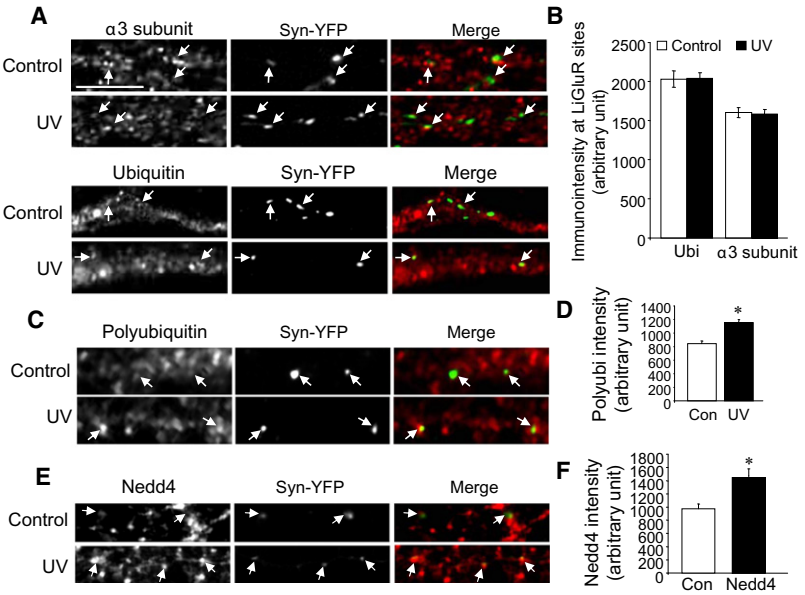

Figure 8. Neuronal Activation Leads to Elevated Distribution of Polyubiquitin and Nedd4 at the LiGluR Synapses

(A and B) LiGluR-expressing cells were stimulated by UV and then immunostained with antibodies against ubiquitin or the 20S proteasome subunit α3. UV stimulation did not alter synaptic accumulation of ubiquitin or proteasomes. Arrows indicate puncta of colocalization.

(C and D) Immunostaining with antibodies specific for polyubiquitin shows higher immunointensity at activated synapses. Arrows indicate puncta of colocalization. *p < 0.05, Student's t test.

(E and F) Immunostaining of E3 ligase Nedd4 following UV stimulation protocol. Nedd4 amount at the LiGluR synapses was increased in UV-treated neurons. Arrows indicate puncta of colocalization. *p < 0.05, Student's t test.

Error bars, mean ± SEM. Scale bar, 5 μm. Con, control. See also Figure S6.

that protein synthesis inhibitors did not block light-induced AMPAR reduction. In contrast, inhibition of proteasomal activity blocked activity-dependent receptor reduction, indicating the involvement of the UPS. Consistent with local regulation of AMPAR turnover, UV stimulation increased levels of the AMPAR E3 ligase Nedd4 and polyubiquitination signals selectively at the activated synapses. These findings support a role of activity-dependent receptor ubiquitination and local degradation; however, an involvement of receptor lateral diffusion cannot be excluded (Borgdorff and Choquet, 2002).

Clearly, the observed response in which prolonged synaptic activity caused a reduction in AMPAR expression represents a negative feedback in nature, consistent with homeostatic synaptic regulation. At single synapses, prolonged suppression of presynaptic neuronal activity results in a homeostatic increase in AMPAR abundance (Hou et al., 2008a; Béïque et al., 2011), indicating the existence of local homeostatic plasticity (Rabinowitch and Segev, 2008; Yu and Goda, 2009; Man, 2011). Thus, the current observation likely represents similar homeostatic regulation at individual synapses. Although homeostatic plasticity is traditionally considered a slow response to long-lasting activity alterations, more recent work indicates that it can be achieved more rapidly, in as short as 1 hr or merely minutes (Aoto et al., 2008; Frank et al., 2006; Ibata et al., 2008; Sutton et al., 2006), comparable to the time course of the present single-synaptic response (30 min).

Global homeostatic plasticity stabilizes the activity of a neuron or a network via limiting the firing rate within an appropriate limit. It has been hypothesized that when a neuron's activity runs out of the physiological range, a primary adjustment is to homeostatically increase or decrease the input strength proportionally across all synapses on the receiving neuron. By employing such synaptic scaling, a neuron is able to maintain the relative synaptic weight, which is considered important for retaining preexisting information. However, with the simultaneous operation of Hebbian plasticity that differentiates synapses into either potentiated or depressed inputs, global synaptic scaling could potentially drive either group of synapses into a runaway status. For instance when widespread LTP inputs drive a neuron into overexcitation (Roth-Alpermann et al., 2006), global downward scaling of inputs onto the neuron could switch some LTD synapses into complete silence, whereas at an LTD dominant cell, upward synaptic scaling could drive the LTP synapses into saturation. Homeostatic responses at single synapses, acting independently or coupled to global homeostatic regulation, could serve as an important regulatory mechanism to eliminate the deleterious situations imposed by Hebbian plasticity and global synaptic scaling.

Over the years a variety of paradigms in homeostatic plasticity has been studied, from which multiple signaling molecules including TNF-α (Stellwagen and Malenka, 2006), Arc (Shepherd et al., 2006), retinoic acid (Aoto et al., 2008), β3-integrin (Cingolani et al., 2008), as well as CDK5 and Polo-like kinase 2 (Seeburg et al., 2008) have been identified. In addition, GluA2-lacking AMPARs, presumably via AMPAR-gated calcium, have also been implicated in homeostatic synaptic regulation (Man, 2011). All of these molecules are implicated in an inactivity-induced homeostatic response, but whether they are utilized in single-synaptic homeostatic regulation remains unclear. Furthermore, in our study prolonged synaptic activation should result in lasting depolarization at the postsynaptic domain, which might be a factor triggering a homeostatic response. However, NMDAR blockade, during which postsynaptic depolarization should remain, is sufficient to abolish AMPAR removal, indicating negligible involvement of local changes in membrane potential. Also, activity of NMDARs is known to stimulate AMPAR internalization to the recycling pathway for reinsertion (Beattie et al., 2000; Ehlers, 2000; Man et al., 2000b, 2007), which is different from current findings that internalized AMPARs seem to be sorted for degradation. Likely, whereas NMDAR activity is necessary, another unidentified molecule, presumably released locally from the activated presynaptic terminal, is also required for single synapse homeostatic regulation on AMPARs.

EXPERIMENTAL PROCEDURES

Primary Hippocampal Neuron Culture

Hippocampal neuron culture was prepared as described previously (Zhang et al., 2009). Briefly, hippocampi were digested, and cells were plated on poly-L-lysine coated coverslips in plating medium. Twenty-four hours after plating, the culture medium was replaced with feeding medium. Thereafter, hippocampal neurons were fed twice a week with 2 ml feeding medium/dish until use.

MAG Application and Illumination

Hippocampal neurons expressing LiGluR were incubated in the dark for 15 min with MAG (10 μM) in ACSF solution containing 150 mM NMDG-HCl, 3 mM KCl, 0.5 mM $CaCl_2$, 5 mM $MgCl_2$, 10 mM HEPES, and 10 mM glucose (pH 7.4). Prior to being transferred to an imaging chamber, cells were rinsed with regular ACSF containing 140 mM NaCl, 10 mM HEPES, 2 mM KCl, 2 mM $CaCl_2$, 1 mM $MgCl_2$, and 5 mM glucose. During imaging experiments the chamber was kept at 37°C with regular ACSF. Illumination was applied using X-Cite −120 fluorescence illumination systems through the 10× objective of an inverted microscope (Zeiss; Axiovert 200M). Photo-switching experiments were carried out with Zeiss microscope shutters. Briefly, light treatment was given as a combination of 0.3 s of blue light (480 nm) followed by 1 s of UV light (380 nm), repeated every 20 s for a certain number of cycles. In control experiments UV light was simply replaced with blue light. Light stimulation cycles were applied automatically by AxioVision imaging software.

Immunocytochemistry

Hippocampal neurons transfected with Lipofectamine 2000 were washed with ACSF and fixed with 4% paraformaldehyde/4% sucrose for 10 min on ice, permeabilized with 0.25% Triton X-100 (on ice, 10 min), or stained without permeabilization for surface labeling. Neurons were blocked with 10% normal goat serum (NGS) in PBS for 1 hr and then incubated with primary antibodies dissolved in 5% NGS/PBS for 2 hr at room temperature. Cells were then washed four times with PBS and incubated with fluorescent Alexa Fluor-conjugated secondary antibodies (1:600) for 1 hr for visualization. For surface staining, live neurons were incubated with antibodies against the extracellular N-terminal of GluA1 (1:100) in culture medium in the incubator for 10 min. Plates were then placed on ice and washed four times with ACSF. After fixation, cells were blocked and incubated with a fluorescent secondary antibody as above.

The following antibodies were used: Alpha3 20S proteasome (1:150; Biomol); bassoon (1:200; Stressgen); GluA1C and GluA1N (1:100; Millipore); GluA2/3 (1:200; homemade); GFP (1:200; Sigma-Aldrich); PSD-95 (1:400; Fisher Scientific); NR1 (1:100; homemade), polyubiquitinated conjugates FK1 (1:100; Enzo); ubiquitin (1:200; Sigma-Aldrich); and Nedd4 (1:200; Abcam).

Imaging

Images were acquired on a Zeiss Axiovert 200M fluorescence microscope using a 63× oil-immersion objective (N.A. 1.4). Immunostained coverslips

were mounted onto slides by using ProLong Gold antifade reagent and kept in the dark for 4 hr before imaging. A DIC snap was first taken for morphological purposes. The exposure time for the fluorescence signal was first set automatically by the software and adjusted manually so that the signals were within the full dynamic range. Either the glow scale look-up table or the histogram was used to monitor the saturation level. Once the parameters were set, they were fixed and used throughout the experiment. For accurate quantification all images were collected in 12 bit gray scale and saved as raw data. Dual channels were used to collect signals from receptor staining (red) and the presynaptic syn-YFP (green).

Local Protein Degradation Assays in Isolated Dendrites

Neurons were transfected with GluA1-GFP at DIV 11 for 3 days. Following a transfer of neurons to a live-imaging chamber maintained at 37°C, dendrites were cleaved manually with a glass micropipette assisted by a micromanipulator, and images were collected with a 40× (N.A. 1.4) oil objective immediately after cleavage and 60 min later. For MG132 blockade, drugs were applied 15 min prior to dendritic cleavage and during imaging. The mean intensity of the isolated and soma-attached dendrites was measured using NIH ImageJ software.

Whole-Cell Patch-Clamp Recording of UV-Induced Neuronal Firing

Neurons were transfected at DIV 11 and patch clamped 2–3 days after transfection; LiGluR agonist MAG was diluted to 10 μM in a bath solution containing 150 mM NMDG-HCl, 3 mM KCl, 0.5 mM $CaCl_2$, 5 mM $MgCl_2$, 10 mM HEPES, and 10 mM glucose (pH 7.4). Neurons were incubated at 37°C in the dark for 15 min, then rinsed with extracellular recording solution containing 140 mM NaCl, 3 mM KCl, 1.5 mM $MgCl_2$, 2.5 mM $CaCl_2$, 11 mM glucose, and 10 mM HEPES (pH 7.4). Patch-clamp recordings were performed using an Axopatch 200B amplifier in the whole-cell current clamp mode. Pipettes had resistances of 3–5 MΩ and were filled with a solution containing 110 mM K-methanesulfonate, 20 mM KCl, 10 mM HEPES, 4 mM Mg-ATP, 0.3 mM Na-GTP, 0.5 mM EGTA, and 10 mM Na-phosphocreatine (pH 7.4). Cells were used for UV stimulation when the resting membrane potential was between −50 and −65 mV.

Illumination was applied using an X-Cite Series 120 light source through the rear port of an inverted microscope (Nikon; Eclipse TE300) using a 40× objective. The physiology rig was fitted with UV (380 nm) and blue (480 nm) filters that were switched manually to illuminate neurons for approximately 1 s with UV or blue light, respectively. Electrophysiological data were recorded and analyzed with pClamp 10 software.

Quantification and Data Analysis

To measure the synaptic content of AMPAR puncta, a double-colored image (red from stained glutamate receptors or other proteins and green signals from syn-YFP) was separated into two channels with NIH ImageJ software. The red channels were thresholded to select AMPAR puncta for quantitative measurement; then the two windows were synchronized. By pointing to a YFP puncta (syn-YFP), indicating a presynaptic terminal from a LiGluR-expressing or syn-YFP control neuron, the corresponding postsynaptic AMPAR cluster was able to be precisely located. Fluorescence intensity of this cluster and those of the neighboring intact clusters were measured. To avoid bias, two or more control clusters were chosen from both sides of the positive synapse in the same dendrite, and the average of the neighboring clusters was used as a control. The AMPAR total intensity of LiGluR synapse was then normalized to the average intensity of neighboring control synapses. Thus, the AMPAR accumulation values represent the difference of AMPAR amounts between activated synapses and the proximal neighboring synapses at the same dendrite. Normally, two to three positive synapses were measured per cell, and 20–30 neurons were analyzed. Statistical significance was determined using Student's t test. All values are reported as mean ± SEM.

SUPPLEMENTAL INFORMATION

Supplemental Information includes six figures and Supplemental Experimental Procedures and can be found with this article online at doi:10.1016/j.neuron.2011.10.011.

ACKNOWLEDGMENTS

We are grateful to Dr. Ehud Isacoff for providing the LiGluR6/MAG system and comments on the manuscripts and Dr. Karl Deisseroth for providing the ChR-2 construct that was used in our initial exploration. We thank H.-Y.M. lab members for helpful discussions and Steve Amato and Amy Lin for critical reading of the manuscript. This work was supported by US National Institutes of Health Grant MH079407 (to H.-Y.M.).

Accepted: October 5, 2011
Published: December 7, 2011

REFERENCES

Aoto, J., Nam, C.I., Poon, M.M., Ting, P., and Chen, L. (2008). Synaptic signaling by all-trans retinoic acid in homeostatic synaptic plasticity. Neuron *60*, 308–320.

Beattie, E.C., Carroll, R.C., Yu, X., Morishita, W., Yasuda, H., von Zastrow, M., and Malenka, R.C. (2000). Regulation of AMPA receptor endocytosis by a signaling mechanism shared with LTD. Nat. Neurosci. *3*, 1291–1300.

Béïque, J.C., Na, Y., Kuhl, D., Worley, P.F., and Huganir, R.L. (2011). Arc-dependent synapse-specific homeostatic plasticity. Proc. Natl. Acad. Sci. USA *108*, 816–821.

Bingol, B., and Schuman, E.M. (2006). Activity-dependent dynamics and sequestration of proteasomes in dendritic spines. Nature *441*, 1144–1148.

Borgdorff, A.J., and Choquet, D. (2002). Regulation of AMPA receptor lateral movements. Nature *417*, 649–653.

Bredt, D.S., and Nicoll, R.A. (2003). AMPA receptor trafficking at excitatory synapses. Neuron *40*, 361–379.

Burrone, J., and Murthy, V.N. (2003). Synaptic gain control and homeostasis. Curr. Opin. Neurobiol. *13*, 560–567.

Burrone, J., O'Byrne, M., and Murthy, V.N. (2002). Multiple forms of synaptic plasticity triggered by selective suppression of activity in individual neurons. Nature *420*, 414–418.

Cingolani, L.A., Thalhammer, A., Yu, L.M., Catalano, M., Ramos, T., Colicos, M.A., and Goda, Y. (2008). Activity-dependent regulation of synaptic AMPA receptor composition and abundance by beta3 integrins. Neuron *58*, 749–762.

Collingridge, G.L., Isaac, J.T., and Wang, Y.T. (2004). Receptor trafficking and synaptic plasticity. Nat. Rev. Neurosci. *5*, 952–962.

Davis, G.W. (2006). Homeostatic control of neural activity: from phenomenology to molecular design. Annu. Rev. Neurosci. *29*, 307–323.

Desai, N.S., Rutherford, L.C., and Turrigiano, G.G. (1999). Plasticity in the intrinsic excitability of cortical pyramidal neurons. Nat. Neurosci. *2*, 515–520.

Ehlers, M.D. (2000). Reinsertion or degradation of AMPA receptors determined by activity-dependent endocytic sorting. Neuron *28*, 511–525.

Ehlers, M.D. (2003). Activity level controls postsynaptic composition and signaling via the ubiquitin-proteasome system. Nat. Neurosci. *6*, 231–242.

Fonseca, R., Vabulas, R.M., Hartl, F.U., Bonhoeffer, T., and Nägerl, U.V. (2006). A balance of protein synthesis and proteasome-dependent degradation determines the maintenance of LTP. Neuron *52*, 239–245.

Frank, C.A., Kennedy, M.J., Goold, C.P., Marek, K.W., and Davis, G.W. (2006). Mechanisms underlying the rapid induction and sustained expression of synaptic homeostasis. Neuron *52*, 663–677.

Goold, C.P., and Nicoll, R.A. (2010). Single-cell optogenetic excitation drives homeostatic synaptic depression. Neuron *68*, 512–528.

Groc, L., and Choquet, D. (2006). AMPA and NMDA glutamate receptor trafficking: multiple roads for reaching and leaving the synapse. Cell Tissue Res. *326*, 423–438.

Grooms, S.Y., Noh, K.M., Regis, R., Bassell, G.J., Bryan, M.K., Carroll, R.C., and Zukin, R.S. (2006). Activity bidirectionally regulates AMPA receptor mRNA abundance in dendrites of hippocampal neurons. J. Neurosci. *26*, 8339–8351.

Hegde, A.N. (2004). Ubiquitin-proteasome-mediated local protein degradation and synaptic plasticity. Prog. Neurobiol. *73*, 311–357.

Hou, Q., Zhang, D., Jarzylo, L., Huganir, R.L., and Man, H.Y. (2008a). Homeostatic regulation of AMPA receptor expression at single hippocampal synapses. Proc. Natl. Acad. Sci. USA *105*, 775–780.

Hou, Q., Huang, Y., Amato, S., Snyder, S.H., Huganir, R.L., and Man, H.Y. (2008b). Regulation of AMPA receptor localization in lipid rafts. Mol. Cell. Neurosci. *38*, 213–223.

Huh, K.H., and Wenthold, R.J. (1999). Turnover analysis of glutamate receptors identifies a rapidly degraded pool of the N-methyl-D-aspartate receptor subunit, NR1, in cultured cerebellar granule cells. J. Biol. Chem. *274*, 151–157.

Ibata, K., Sun, Q., and Turrigiano, G.G. (2008). Rapid synaptic scaling induced by changes in postsynaptic firing. Neuron *57*, 819–826.

Ju, W., Morishita, W., Tsui, J., Gaietta, G., Deerinck, T.J., Adams, S.R., Garner, C.C., Tsien, R.Y., Ellisman, M.H., and Malenka, R.C. (2004). Activity-dependent regulation of dendritic synthesis and trafficking of AMPA receptors. Nat. Neurosci. *7*, 244–253.

Juo, P., and Kaplan, J.M. (2004). The anaphase-promoting complex regulates the abundance of GLR-1 glutamate receptors in the ventral nerve cord of C. elegans. Curr. Biol. *14*, 2057–2062.

Kato, A., Rouach, N., Nicoll, R.A., and Bredt, D.S. (2005). Activity-dependent NMDA receptor degradation mediated by retrotranslocation and ubiquitination. Proc. Natl. Acad. Sci. USA *102*, 5600–5605.

Kim, M.J., Dunah, A.W., Wang, Y.T., and Sheng, M. (2005). Differential roles of NR2A- and NR2B-containing NMDA receptors in Ras-ERK signaling and AMPA receptor trafficking. Neuron *46*, 745–760.

Lee, H.K., Kameyama, K., Huganir, R.L., and Bear, M.F. (1998). NMDA induces long-term synaptic depression and dephosphorylation of the GluR1 subunit of AMPA receptors in hippocampus. Neuron *21*, 1151–1162.

Lee, S.H., Simonetta, A., and Sheng, M. (2004). Subunit rules governing the sorting of internalized AMPA receptors in hippocampal neurons. Neuron *43*, 221–236.

Lee, M.C., Yasuda, R., and Ehlers, M.D. (2010). Metaplasticity at single glutamatergic synapses. Neuron *66*, 859–870.

Lévi, S., Schweizer, C., Bannai, H., Pascual, O., Charrier, C., and Triller, A. (2008). Homeostatic regulation of synaptic GlyR numbers driven by lateral diffusion. Neuron *59*, 261–273.

Lin, A., Hou, Q., Jarzylo, L., Amato, S., Gilbert, J., Shang, F., and Man, H.Y. (2011). Nedd4-mediated AMPA receptor ubiquitination regulates receptor turnover and trafficking. J. Neurochem. *119*, 27–39.

Lin, J.W., Ju, W., Foster, K., Lee, S.H., Ahmadian, G., Wyszynski, M., Wang, Y.T., and Sheng, M. (2000). Distinct molecular mechanisms and divergent endocytotic pathways of AMPA receptor internalization. Nat. Neurosci. *3*, 1282–1290.

Lu, W., Man, H., Ju, W., Trimble, W.S., MacDonald, J.F., and Wang, Y.T. (2001). Activation of synaptic NMDA receptors induces membrane insertion of new AMPA receptors and LTP in cultured hippocampal neurons. Neuron *29*, 243–254.

Lussier, M.P., Nasu-Nishimura, Y., and Roche, K.W. (2011). Activity-dependent ubiquitination of the AMPA receptor subunit GluA2. J. Neurosci. *31*, 3077–3081.

Maffei, A., and Fontanini, A. (2009). Network homeostasis: a matter of coordination. Curr. Opin. Neurobiol. *19*, 168–173.

Malenka, R.C. (2003). Synaptic plasticity and AMPA receptor trafficking. Ann. N Y Acad. Sci. *1003*, 1–11.

Malinow, R., and Malenka, R.C. (2002). AMPA receptor trafficking and synaptic plasticity. Annu. Rev. Neurosci. *25*, 103–126.

Mammen, A.L., Huganir, R.L., and O'Brien, R.J. (1997). Redistribution and stabilization of cell surface glutamate receptors during synapse formation. J. Neurosci. *17*, 7351–7358.

Man, H.Y. (2011). GluA2-lacking, calcium-permeable AMPA receptors—inducers of plasticity? Curr. Opin. Neurobiol. *21*, 291–298.

Man, H.Y., Sekine-Aizawa, Y., and Huganir, R.L. (2007). Regulation of alpha-amino-3-hydroxy-5-methyl-4-isoxazolepropionic acid receptor trafficking through PKA phosphorylation of the Glu receptor 1 subunit. Proc. Natl. Acad. Sci. USA *104*, 3579–3584.

Man, H.Y., Ju, W., Ahmadian, G., and Wang, Y.T. (2000a). Intracellular trafficking of AMPA receptors in synaptic plasticity. Cell. Mol. Life Sci. *57*, 1526–1534.

Man, H.Y., Wang, Q., Lu, W.Y., Ju, W., Ahmadian, G., Liu, L., D'Souza, S., Wong, T.P., Taghibiglou, C., Lu, J., et al. (2003). Activation of PI3-kinase is required for AMPA receptor insertion during LTP of mEPSCs in cultured hippocampal neurons. Neuron *38*, 611–624.

Man, H.Y., Lin, J.W., Ju, W.H., Ahmadian, G., Liu, L., Becker, L.E., Sheng, M., and Wang, Y.T. (2000b). Regulation of AMPA receptor-mediated synaptic transmission by clathrin-dependent receptor internalization. Neuron *25*, 649–662.

Marder, E., and Goaillard, J.M. (2006). Variability, compensation and homeostasis in neuron and network function. Nat. Rev. Neurosci. *7*, 563–574.

Nakayama, K., Kiyosue, K., and Taguchi, T. (2005). Diminished neuronal activity increases neuron-neuron connectivity underlying silent synapse formation and the rapid conversion of silent to functional synapses. J. Neurosci. *25*, 4040–4051.

Newpher, T.M., and Ehlers, M.D. (2008). Glutamate receptor dynamics in dendritic microdomains. Neuron *58*, 472–497.

Park, M., Penick, E.C., Edwards, J.G., Kauer, J.A., and Ehlers, M.D. (2004). Recycling endosomes supply AMPA receptors for LTP. Science *305*, 1972–1975.

Patrick, G.N., Bingol, B., Weld, H.A., and Schuman, E.M. (2003). Ubiquitin-mediated proteasome activity is required for agonist-induced endocytosis of GluRs. Curr. Biol. *13*, 2073–2081.

Pozo, K., and Goda, Y. (2010). Unraveling mechanisms of homeostatic synaptic plasticity. Neuron *66*, 337–351.

Rabinowitch, I., and Segev, I. (2008). Two opposing plasticity mechanisms pulling a single synapse. Trends Neurosci. *31*, 377–383.

Rich, M.M., and Wenner, P. (2007). Sensing and expressing homeostatic synaptic plasticity. Trends Neurosci. *30*, 119–125.

Roth-Alpermann, C., Morris, R.G., Korte, M., and Bonhoeffer, T. (2006). Homeostatic shutdown of long-term potentiation in the adult hippocampus. Proc. Natl. Acad. Sci. USA *103*, 11039–11044.

Royer, S., and Paré, D. (2003). Conservation of total synaptic weight through balanced synaptic depression and potentiation. Nature *422*, 518–522.

Schwarz, L.A., Hall, B.J., and Patrick, G.N. (2010). Activity-dependent ubiquitination of GluA1 mediates a distinct AMPA receptor endocytosis and sorting pathway. J. Neurosci. *30*, 16718–16729.

Seeburg, D.P., Feliu-Mojer, M., Gaiottino, J., Pak, D.T., and Sheng, M. (2008). Critical role of CDK5 and Polo-like kinase 2 in homeostatic synaptic plasticity during elevated activity. Neuron *58*, 571–583.

Segref, A., and Hoppe, T. (2009). Think locally: control of ubiquitin-dependent protein degradation in neurons. EMBO Rep. *10*, 44–50.

Shen, H., Korutla, L., Champtiaux, N., Toda, S., LaLumiere, R., Vallone, J., Klugmann, M., Blendy, J.A., Mackler, S.A., and Kalivas, P.W. (2007). NAC1 regulates the recruitment of the proteasome complex into dendritic spines. J. Neurosci. *27*, 8903–8913.

Sheng, M., and Hyoung Lee, S. (2003). AMPA receptor trafficking and synaptic plasticity: major unanswered questions. Neurosci. Res. *46*, 127–134.

Shepherd, J.D., Rumbaugh, G., Wu, J., Chowdhury, S., Plath, N., Kuhl, D., Huganir, R.L., and Worley, P.F. (2006). Arc/Arg3.1 mediates homeostatic synaptic scaling of AMPA receptors. Neuron *52*, 475–484.

Song, I., and Huganir, R.L. (2002). Regulation of AMPA receptors during synaptic plasticity. Trends Neurosci. *25*, 578–588.

Stellwagen, D., and Malenka, R.C. (2006). Synaptic scaling mediated by glial TNF-alpha. Nature *440*, 1054–1059.

Steward, O., and Schuman, E.M. (2001). Protein synthesis at synaptic sites on dendrites. Annu. Rev. Neurosci. *24*, 299–325.

Steward, O., and Schuman, E.M. (2003). Compartmentalized synthesis and degradation of proteins in neurons. Neuron *40*, 347–359.

Sutton, M.A., Wall, N.R., Aakalu, G.N., and Schuman, E.M. (2004). Regulation of dendritic protein synthesis by miniature synaptic events. Science *304*, 1979–1983.

Sutton, M.A., Ito, H.T., Cressy, P., Kempf, C., Woo, J.C., and Schuman, E.M. (2006). Miniature neurotransmission stabilizes synaptic function via tonic suppression of local dendritic protein synthesis. Cell *125*, 785–799.

Szobota, S., Gorostiza, P., Del Bene, F., Wyart, C., Fortin, D.L., Kolstad, K.D., Tulyathan, O., Volgraf, M., Numano, R., Aaron, H.L., et al. (2007). Remote control of neuronal activity with a light-gated glutamate receptor. Neuron *54*, 535–545.

Tanaka, J., Horiike, Y., Matsuzaki, M., Miyazaki, T., Ellis-Davies, G.C., and Kasai, H. (2008). Protein synthesis and neurotrophin-dependent structural plasticity of single dendritic spines. Science *319*, 1683–1687.

Tian, L., Hires, S.A., Mao, T., Huber, D., Chiappe, M.E., Chalasani, S.H., Petreanu, L., Akerboom, J., McKinney, S.A., Schreiter, E.R., et al. (2009). Imaging neural activity in worms, flies and mice with improved GCaMP calcium indicators. Nat. Methods *6*, 875–881.

Turrigiano, G.G. (2008). The self-tuning neuron: synaptic scaling of excitatory synapses. Cell *135*, 422–435.

Turrigiano, G.G., and Nelson, S.B. (1998). Thinking globally, acting locally: AMPA receptor turnover and synaptic strength. Neuron *21*, 933–935.

Turrigiano, G.G., Leslie, K.R., Desai, N.S., Rutherford, L.C., and Nelson, S.B. (1998). Activity-dependent scaling of quantal amplitude in neocortical neurons. Nature *391*, 892–896.

Wierenga, C.J., Ibata, K., and Turrigiano, G.G. (2005). Postsynaptic expression of homeostatic plasticity at neocortical synapses. J. Neurosci. *25*, 2895–2905.

Yu, L.M., and Goda, Y. (2009). Dendritic signalling and homeostatic adaptation. Curr. Opin. Neurobiol. *19*, 327–335.

Zhang, D., Hou, Q., Wang, M., Lin, A., Jarzylo, L., Navis, A., Raissi, A., Liu, F., and Man, H.Y. (2009). Na,K-ATPase activity regulates AMPA receptor turnover through proteasome-mediated proteolysis. J. Neurosci. *29*, 4498–4511.